

**Breaking limit of atomic distance in an impurity-free monatomic chain**

Chang Q. Sun,\* C. M. Li, S. Li, and B. K. Tay

*School of Electrical and Electronic Engineering, Nanyang Technological University, Singapore 639798, Singapore*

(Received 8 January 2004; revised manuscript received 15 March 2004; published 9 June 2004)

An analytical solution shows that the maximal strain of an impurity-free metallic monatomic chain (MC), or a defect-free nanowire (NW), varies inapparently with mechanical stress but apparently with the separation between the melting point [ $T_m(K)$ ] and the temperature of operation in terms of  $\exp\{[T_m(K)-T]^{-1}\}$ , where  $K$  is the dimension of the NW (for a MC,  $K=1.5$ ). Reconciliation of the measured data of Au-MC breaking limit suggests that the discrepancy in measurement arises from thermal and mechanical fluctuations near the  $T_m$  of the MC that is (1/4.2)-fold of the bulk value. Findings also favor the mechanism for the high extensibility of a nanograined NW and further indicate that bond unfolding of the lower-coordinated atoms dominates the grain boundary activities, particularly at temperatures approaching surface melting.

DOI: 10.1103/PhysRevB.69.245402

PACS number(s): 81.40.Jj, 61.46.+w

**I. INTRODUCTION**

Metallic monatomic chains (MC's) and nanowires (NW's) have attracted tremendous interest because of their fundamental significance and fascinating properties such as quantum conductance, chemical reactivity, thermal stability, mechanical strength, and ductility. These are key issues of concern in upcoming technologies such as nanodevices. A metallic MC is an ideal prototype for extensibility study, as the MC involves merely bond stretching without bond unfolding or atomic gliding dislocations, as do atoms in a metallic NW consisting of nanograins upon being stretched.<sup>1</sup> Measured using transmission electron microscopy (TEM) at room temperature under tension, the Au-Au bond breaks at a length that varies from 0.29 nm,<sup>2</sup> 0.36 nm ( $\pm 30\%$ ),<sup>3</sup> 0.35–0.40 nm (Ref. 4) to even a single event of 0.48 nm,<sup>5</sup> while at 4.2 K the breaking limit is reduced to  $0.23 \pm 0.04$  nm as measured using scanning tunneling microscopy and mechanically controlled break junction.<sup>6</sup> Sophisticated calculations suggest that the Au-Au equilibrium distance (without external stimulus) contracts to a range between 0.232 and 0.262 nm (Ref. 7) from the bulk value, 0.2878 nm, whereas the maximal Au-Au distance under tension does not exceed 0.31 nm.<sup>8</sup> The Au-Au bond in the MC is twice stronger than that in the bulk.<sup>9</sup> The discrepancy could not be theoretically solved without inserting impurity atoms such as H, B, C, N, O, and S into the Au-Au chain in calculations.<sup>10</sup> Metallic NW's such as Cu and Al show an extensibility that is one to three orders higher than the bulk values though the MC's of Cu and Al are hard to form at ambient temperature. The high extensibility was attributed to atomic dislocations or atomic diffusion at grain boundaries that are suggested to be easier.<sup>11,12</sup>

Combining the effects of thermal expansion, mechanical stretching, and the atomic coordination-number (CN) imperfection caused bond contraction with the fact that a molten phase is extremely compressible, we have derived a numerical solution to solve the discrepancy in atomic separation of an impurity-free MC with and without thermal and mechanical stimuli. Extension of the solution to a defect-free metallic NW suggests that bond unfolding or atomic sliding of the

lower-coordinated atoms at grain boundaries dominates the high extensibility of a nanograined NW at temperatures close to that for surface melting.

**II. THEORY**

The bond-order-length-strength (BOLS) correlation premise, which has been detailed in Ref. 13, indicates that the CN imperfection of atoms at sites surrounding defects or near the surface edge causes the remaining bonds of the lower-coordinated atoms to contract spontaneously, associated with strengthening of the shortened bond. The bond strengthening contributes to the Hamiltonian that dictates the entire band structure such as the core-level shift and<sup>13</sup> band-gap expansion.<sup>14</sup> On the other hand, the atomic CN imperfection lowers the atomic cohesive energy that dominates the thermal stability such as melting<sup>20</sup> and phase transition<sup>15,16</sup> and determines the activation energy for atomic diffusion, atomic dislocation, and chemical reaction. The competition between energy density elevation and the atomic cohesive energy suppression in the relaxed region dominates the mechanical strength and compressibility of a nanosolid.<sup>17</sup> The BOLS correlation has also enabled us to determine the identities of a C-C bond in carbon nanotubes,<sup>17</sup> the energy levels of an isolated atom,<sup>13</sup> and the vibration frequency of a Si-Si dimer bond.<sup>18</sup> Matching the BOLS predictions to the measurements reveals that at the lower end of the size limit (one unit cell with atomic CN of 2), the Au 4*f*-level binding energy increases by  $\sim 43\%$  ( $=c_i^{-1}-1$ ) with respect to the bulk value of  $-2.87$  eV and the melting point of the smallest Au nanosolid, or the Au-MC, decreases from 1337.33 K to 320 K, which is 1/4.2 times the bulk value.<sup>19</sup>

Figure 1 illustrates schematically the BOLS correlation using the pairwise interatomic potential. When the CN of an atom is reduced, the equilibrium atomic distance will contract from 1 (unit in  $d$ , being the equilibrium bond length in the bulk) to  $c_i$  and the bond energy will increase in magnitude from 1 (unit in  $E_b$ , being the cohesive energy per bond in the bulk) to  $c_i^{-m}$ . The  $c_i$  is the bond contraction coefficient. The index  $m$  is an adjustable parameter depending on the nature of the bond. For metals,  $m=1$ ; for Si and C,  $m$  has

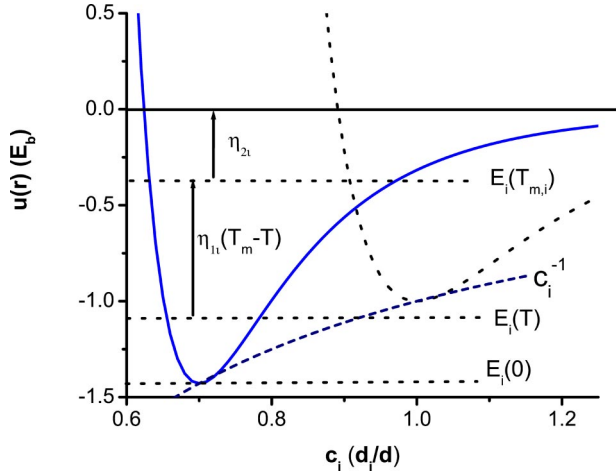


FIG. 1. Schematic illustration of the BOLS correlation for a MC. CN imperfection causes the bond to contract from 1 unit (in  $d$ ) to 0.6973 and the cohesive energy per coordinate increases by  $c_i^{-1}$  from 1 unit (in  $E_b$ ) to 1.43. Separation between  $E_i(T)$  and  $E_i(0)$  is the thermal vibration energy. Separation between  $E_i(T_{m,i})$  and  $E_i(T)$  corresponds to the energy needed for melting.  $T_{m,i}$  is the melting point. The energy required to break the bond at  $T$  is the separation between zero and  $E_i(T)$ , or  $\eta_{1i}(T_{m,i}-T) + \eta_{2i}$ .

been optimized to be 4.88 (Ref. 13) and 2.67,<sup>17</sup> respectively. The solid and the dotted  $u(r)$  curves correspond to the pairwise interatomic potential with and without CN imperfection. The BOLS correlation discussed herein is consistent with the trend reported in Ref. 7, albeit the extent of bond contraction and energy enhancement varies from case to case in Ref. 7. The BOLS correlation formulates the bond length  $d_i$ , the bond energy  $E_i(T=0)$ , and the cohesive energy  $E_{Bi}$ , per atom in the MC in the following forms:<sup>13-15</sup>

$$\begin{aligned} d_i(z_i)/d &= c_i(z_i) = 2/\{1 + \exp[(12 - z_i)/8z_i]\} \\ &= 0.6973 \quad (z_i = 2), \end{aligned}$$

$$E_i(T=0) = c_i^{-1}E_b(T=0) \cong 1.5E_b,$$

$$T_{m,i} \propto E_{Bi} = z_i E_i, \quad (1)$$

where  $z_i$  is the effective atomic CN.  $T_{m,i}$ , the melting point of the MC, is proportional to the atomic cohesive energy  $E_{Bi} = z_i E_i$ .<sup>20,21</sup> Subscripts  $i$  and  $b$  denote a specific  $i$ th atom in the MC and an atom in the bulk. The BOLS premise predicts that an Au-MC ( $z_i=2$ ) bond contracts by  $1 - 0.6973 \cong 30\%$  from 0.2878 to 0.2007 nm and the bond strength ( $E_i/d_i = c_i^{-2} \sim 2$ ) becomes two times the bulk value. The predicted Au-MC equilibrium length is slightly shorter than that measured under tension at 4.2 K,  $0.23 \pm 0.04$  nm,<sup>6</sup> and the predicted bond strength agrees with reported values.<sup>9</sup> Such consistencies further evidence the validity of the BOLS consideration that attributes the size dependency of a nanosolid to the atomic CN imperfection and the increased portion of the low-CN atoms of the nanosolid.

The characteristic energies as indicated in Fig. 1 represent the following.

(i) at  $E=0$ , the bond is completely broken with zero interatomic interaction.

(ii) Separation between  $E=0$  and  $E_i(T)$  is the cohesive energy per CN at  $T$ , which is the energy required for bond breaking.

(iii) The spacing between  $E_i(T)$  and  $E_i(0)$  is the energy of thermal vibration. If one wants to melt an atom with  $z_i$  coordinates by heating the system from  $T$  to  $T_{m,i}$ , one needs to provide  $z_i[E_i(T_{m,i}) - E_i(T)] = z_i \eta_{1i}(T_{m,i} - T)$  energy. When  $T$  approaches  $T_{m,i}$ , the mechanical strength approaches zero with infinite compressibility.

One may apply a tensile stress  $P$  to stretch a bond in the MC from its original equilibrium length at  $T$ ,  $d_i(z_i, T, 0)$ , to the breaking limit,  $d_{iM}(z_i, T, P)$ . Mechanically rupturing of the bond at temperature  $T$  needs energy  $\eta_{1i}(T_{m,i} - T) + \eta_{2i}$  that equals the  $(1/z_i)$ -fold thermal energy for evaporating an atom in solid state at  $T$ ,

$$\begin{aligned} \int_{d_i(z_i, T, 0)}^{d_{iM}(z_i, T, P)} P(x) dx &= \bar{P}[d_{iM}(z_i, T, P) - d_i(z_i, T, 0)] = \bar{P} \Delta d_i \\ &\propto \eta_{1i}(T_{m,i} - T) + \eta_{2i}. \end{aligned} \quad (2)$$

Ideally, the slope  $\eta_{1i}$  corresponds to the specific heat per coordinate. The constant  $\eta_{2i}$  represents  $(1/z_i)$ -fold energy required for evaporating a molten atom of the MC.  $\eta_{1i}$  and  $\eta_{2i}$  can be determined with the known  $c_i^{-m}$  and the corresponding bulk values of  $\eta_{1b}$  and  $\eta_{2b}$  that have been obtained as shown in Ref. 22 in detail.

Considering the effects of atomic CN-imperfection-induced bond contraction ( $c_i d$ ), thermal expansion ( $1 + \alpha T$ , with  $\alpha$  being the linear coefficient), and mechanical stretching [ $1 + \beta_i(z_i, T)P$ , with coefficient  $\beta_i$ ], the distance between two nearest atoms in the interior of a MC can be expressed as

$$d_i(z_i, T, P) = d \times c(z_i)(1 + \alpha T)[1 + \beta_i(z_i, T)P].$$

The maximal strain is then expressed as

$$\frac{\Delta d_{iM}(z_i, T, P)}{d_i(z_i, T, 0)} = \beta_i(z_i, T) \bar{P}, \quad (3)$$

here  $d_i(z_i, T, 0) = d \times c(z_i)(1 + \alpha T)$  is the bond length at  $T$  without being stretched. One can approximate the mean  $\bar{P}$  to the  $P(x)$  in Eqs. (2) and (3), as the  $d_{iM}(z_i, T, P)$  represents the breaking limit and the integration is a constant. Combining Eqs. (2) and (3), one has

$$\bar{P} = \pm \left\{ \frac{\eta_{1i}(T_{m,i} - T) + \eta_{2i}}{\beta_i(z_i, T) \times d_i(z_i, T, 0)} \right\}^{1/2}. \quad (4)$$

For tensile stress,  $\bar{P} > 0$ , for compressive stress,  $\bar{P} < 0$ . The extensibility or compressibility  $\beta$  of a system is expressed as<sup>23</sup>

$$\begin{aligned} \beta_i(z_i, T) &= - \left. \frac{\partial V}{V \partial P} \right|_T = \left. \left[ -V \frac{\partial^2 u(r, T)}{\partial V^2} \right]^{-1} \right|_T \\ &\propto \frac{d_i^{\tau}(z_i, T, 0)}{N_i[E_i(T_{m,i}) - E_i(T)]} \propto \frac{d_i^{\tau}(z_i, T, 0)}{\eta_{1i}(T_{m,i} - T)}. \end{aligned} \quad (5)$$

$\beta$  is the inverse of Young's modulus or hardness in a dimen-

sion that equals the sum of bond energy per unit volume.<sup>24</sup> The power index  $\tau=1, 2$ , and 3 corresponds to the dimensionality of a MC, a rod, and a spherical dot.  $N_i$  is the total number of bonds in  $d_i^\tau$  volume. One needs to note that the bond number density in the relaxed region does not change upon relaxation. For instance, bond relaxation never changes the bond number between the neighboring atoms in a MC, whether the MC is suspended or embedded in the bulk. Thus, the temperature dependent extensibility of a MC is reduced with the bulk value at  $T=0$  as

$$\frac{\beta_i(z_i, T)}{\beta_0(z_b, 0)} = \frac{\eta_{1b} d_i(z_i, T, 0)}{\eta_{1i} d} \left( \frac{T_{m,b}}{T_{m,i} - T} \right) = \frac{\eta_{1b} c_i (1 + \alpha x T_{m,b})}{\eta_{1i} (x_{m,i} - x)}. \quad (6)$$

The dimensionless  $x_{m,i}$  and  $x$  are the  $T_{m,i}$  and  $T$  reduced by the bulk  $T_{m,b}$ , and they satisfy  $x < x_{m,i} \leq 1$ . When the  $T$  approaches the  $T_{m,i}$ , the compressibility is singular, which may represent the true situation that a molten phase is highly compressible. Substituting Eqs. (4) and (6) into Eq. (3) yields

$$\begin{aligned} \frac{\Delta d_{iM}(z_i, T, P)}{d_i(z_i, T, 0)} &= \beta_i(z_i, T) \bar{P} \\ &= \left\{ \frac{\beta(z_i, T) \times [\eta_{1i}(T_{m,i} - T) + \eta_{2i}]}{d_i(z_i, T, 0)} \right\}^{1/2} \\ &= \left[ \frac{\eta_{1b} d_i(z_i, T, 0) \times \beta_0(z_b, 0)}{\eta_{1i} d \times d_i(z_i, T, 0)} \right. \\ &\quad \times \left. \left( \frac{T_{m,b}}{T_{m,i} - T} \right) [\eta_{1i}(T_{m,i} - T) + \eta_{2i}] \right]^{1/2} \\ &= \left[ \frac{\beta_0 \eta_{1b} T_{m,b}}{d} \left( 1 + \frac{\eta_{2i}}{\eta_{1i}(T_{m,i} - T)} \right) \right]^{1/2} \\ &\cong \left( \frac{\beta_0 \eta_{1b} T_{m,b}}{d} \right)^{1/2} \exp \left\{ \frac{\eta_{2i}}{2 \eta_{1i} [T_{m,i} - T]} \right\} \\ &= A \exp \left\{ \frac{\eta_{2i}}{2 \eta_{1i} T_{m,b} [x_{m,i} - x]} \right\}. \quad (7) \end{aligned}$$

For a metallic MC with  $z_i=2$ ,  $T_{m,i}=T_{m,b}/4.2$ . The analytical expression of the maximal strain varies inapparently with  $P$  or the strain rate but apparently with the separation between  $x_{m,i}$  and  $x$ . The prefactor  $A$  is material nature dependent and the  $\eta_{2i}/\eta_{1i}$  ratio is crystal structure dependent.<sup>22</sup>

If the  $x_{m,i}$  and the  $\eta_{2i}/\eta_{1i}$  ratio are replaced with the size-dependent  $x_m(K)$  and  $\eta_2(K)/\eta_1(K)$ , the extensibility/compressibility and the strain limit of a defect-free nanosolid become

$$\begin{aligned} \frac{\Delta \beta_i(z_i, T)}{\beta_0(z_b, 0)} &= \frac{\eta_{1b} c^\tau(K) (1 + \alpha x T_{m,b})}{\eta_1(K) [x_m(K) - x]} - 1, \\ \frac{\Delta d_M(K, T, P)}{d(K, T, 0)} &= A \exp \left\{ \frac{\eta_2(K)}{2 \eta_1(K) T_{m,b} [x_m(K) - x]} \right\}, \\ c(K) &= 1 + \sum_3 \gamma_i (c_i - 1), \end{aligned}$$

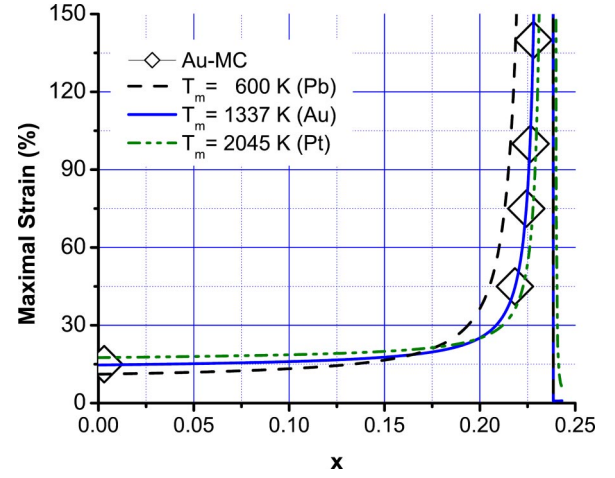


FIG. 2. Temperature ( $x=T/T_{m,b}$ ) dependence of a MC breaking limit in comparison with values for an Au-MC measured at 4 K ( $0.23 \pm 0.04$  nm) and at ambient ( $298 \pm 6$  K,  $0.29 \sim 0.48$  nm) indicates that the scattered data arise from thermal and mechanical fluctuations near the melting point of the Au-MC which is around 320 K. Varying the  $T_{m,b}$  changes slightly the easiness of MC bond breaking at different temperatures.

$$x_m(K) = 1 + \sum_3 \gamma_i (z_{ib} c_i^{-m} - 1), \quad (8)$$

where  $\gamma_i \sim \tau c_i / K$  is the portion of atoms in the  $i$ th atomic layer and the  $i$  is counted from the outermost layer to the center of the solid up to three.<sup>13</sup> The  $x_m(K)$  is dominated by the relative change of atomic cohesive energy, and  $c(K) = d(K)/d$  is the coefficient of mean lattice contraction.<sup>20,25</sup>

### III. RESULTS AND DISCUSSION

#### A. Monatomic chain

In order to examine the validity of the prediction, we introduced  $\alpha = 14.7 \times 10^{-6}$ ,  $T_{m,b} = 1337.33$  K,  $d = 0.2878$  nm in Eq. (7) to solve the equation for an Au-MC. The measured breaking limits of  $d_{iM}(4 \text{ K}) = 0.23$  nm,<sup>6,7</sup> and the mean  $d_{iM}(300 \text{ K}) = 0.35$  nm (Refs. 2–4) were used, which leads to the quantification of the two unknown parameters as  $\beta_0 = 0.005 \text{ GPa}^{-1}$  and  $\eta_{2i}/\eta_{1i} = 64$  K. Noting the relation  $E_i = c_i^{-1} E_b$ , and hence,  $\eta_{1i} T_{m,i} + \eta_{2i} = c_i^{-1} (\eta_{1b} T_{m,b} + \eta_{2b})$ , with the given  $\eta_{1b} = 0.000 554 2 \text{ eV/K}$  and  $\eta_{2b} = -0.24 \text{ eV}$  for the fcc structures,<sup>22</sup>  $\eta_{1i} = 0.001 87 \text{ eV/K} \sim 3 \eta_{1b}$ , and  $\eta_{2i} = 0.1197 \text{ eV}$  were obtained. The  $\eta_{2b} < 0$  in Ref. 22 means that the actual energy for evaporating the molten atom is included in the  $\eta_{1b} T_m$  term, and therefore, the  $\eta_{1b}$  there may exaggerate the specific heat per coordinate. Accuracy of solutions is subject strictly to the  $\eta_{1b}$  and  $\eta_{2b}$  values and the precision of the measured two  $d_{iM}(T \neq 0)$  values for calibration, as no freely adjustable parameters are involved. Figure 2 compares the calculated curves with the measured maximal strains for an Au-MC at various temperatures. Excitingly, the theoretical curve covers all the divergent values measured at 4 K ( $0.23 \pm 0.04$  nm) and at ambient temperature ( $298 \pm 6$  K,  $0.29 \sim 0.48$  nm). The divergent data are centered



at some 22 K below the MC melting point, 320 K ( $x = 1/4.2$ ), with 6 K fluctuation. Finding herewith shows clearly now that the divergent values of breaking limit measured at ambient originate from thermal and mechanical fluctuations near the melting point of the MC that is 1/4.2 fold of the bulk value rather than impurity meditation.

Figure 2 also suggests that the dominant factor  $T_{m,b}$  has slight influences on the breaking mode of a MC. The bond of a low- $T_{m,b}$  specimen breaks more readily at low temperature than the bond of a high- $T_{m,b}$  element; the bond of the low- $T_{m,b}$  specimen is more easily extended at  $T$  approaching the  $T_{m,i}$  and the operating  $x$  should be slightly lower than the high- $T_{m,b}$  material. It is anticipated that a metallic MC could form only at a temperature that is 20–30 K lower than the value of  $T_{m,b}/4.2$ . For instance, if one wants to make a MC at 300 K of a certain specimen, one has to work with the material whose  $T_{m,b} = (300 + 20) \times 4.2 = 1344$  K or around. This also explains why not all the metals could form MC at ambient temperature and suggests that one may need to operate at a proper temperature to make the specific MC. Therefore, it is not surprising that Au is favorable for MC formation at ambient temperature whereas Ag ( $T_{m,b} = 1235$  K), Al ( $T_{m,b} = 933.5$  K), and Cu ( $T_{m,b} = 1356$  K, only 20 K higher than the  $T_{m,b}$  of Au) do not (or to a very limited extent) have this property, though they could form NW's with high extensibility.<sup>33</sup> Although the electron structure may need to be considered in making a MC,<sup>26</sup> we suggest that the operating temperature would be critical in making a MC.

### B. Nanowires

Understanding may provide insight into the extensibility of metallic NW's, such as Cu and Al NW's, that could form at room temperature or subambient temperature.<sup>11,12</sup> Figure 3 shows counterplots for the size and  $x$  dependent extensibility and maximal strain of Au-NW's with the parameters determined for the Au-MC. The  $\alpha T_{m,b} \cong 3-5\%$  is negligible. The ratio  $\eta_{1b}/\eta_1(K) = 1 + 4/\{1 + \exp[(K-1.5)/20]\}$  is assumed to change from 1/3 (at  $K=1.5$ ) to 1 (at  $K=\infty$ ) gradually. For a NW,  $\tau=2$ . Note that the  $c(K)$  drops from 1 to 0.7, and the  $x_m(K)$  drops from 1 to 1/4.2 when a NW of infinite size shrinks to a MC. Equation (8) indicates that the extensibility enhancement happens when  $[x_m(K) - x] < c^\tau(K) \eta_{1b}/\eta_1(K)$ , otherwise, the extensibility is lower than the bulk value. When the  $x_m(K)$  approaches  $x$ , the extensibility increases rapidly and then approaches infinity at  $x \sim x_m(K)$ . Nevertheless, measurements have shown in Fig. 2 that the detectable maximal strain of a suspended Au-MC bond is less than 150%. Both the extensibility and the maximal strain are much lower than the detected strain ( $10^3$ ) of a nanograined NW.<sup>1</sup> This indicates that bond stretching we discussed herein is not the factor that dominates the high extensibility of a NW. Therefore, the mechanism<sup>1,11,12,27</sup> of atomic gliding dislocations and grain boundary movement is highly favored. We further suggest that the barrier or activation energy for atomic dislocation and diffusion of a lower coordinated atom at the grain boundaries is lower than that of a fully coordinated atom in the bulk, as these activities are subject to atomic cohesion that drops with atomic CN.

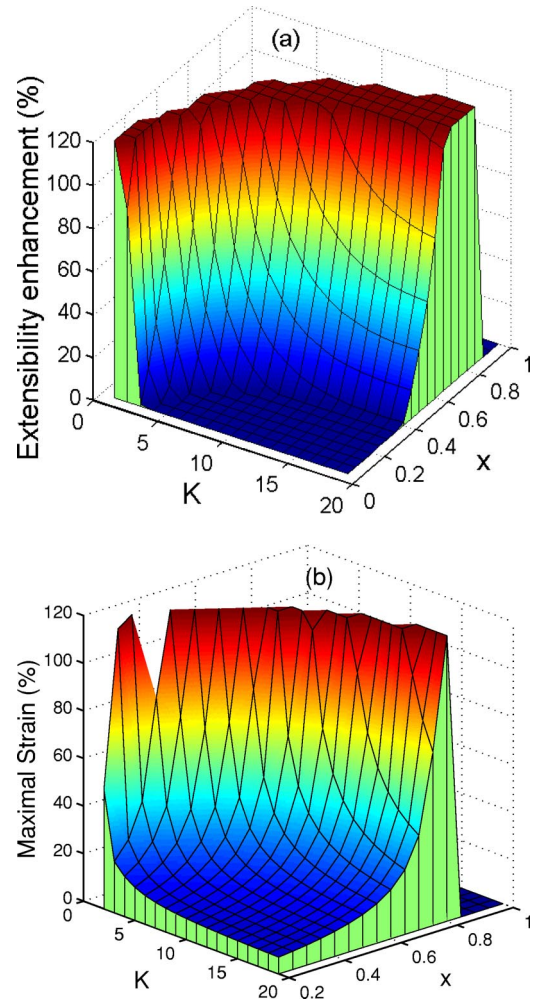


FIG. 3. Illustrative counterplots for the size ( $K=D/2d$ ) and  $x$  dependent extensibility and maximal strain of defect-free Au-NW's. The extensibility and the maximal strain increase rapidly when  $x$  approaches  $x_m(K)$  that drops with  $K$ .

One may note that the lower-coordinated atoms in the outermost atomic layers dominate the extensibility as the melting of a nanosolid starts from the surface and extends to the next shell when the temperature is raised.<sup>28,29</sup> At temperatures close to the  $T_{m,1}$  of the surface, the maximal strain and the extensibility of the surface layer approach infinity. At these temperatures or above, bond breaking under tension should start from the NW interior, because the inner bonds first reach their strain limits. However, at temperatures far below the  $T_{m,1}$ , bond breaking may start from the outermost atomic shell and nanosolid manifests brittle characteristics, as the shortened surface bonds break first. Therefore, the breaking of a NW at different temperatures is expected to be in different modes. On the other hand, thermal energy released from bond breaking and bond unfolding should add energy to the system by raising the actual temperature of the NW. Furthermore, electron bombardment during the TEM measurement also raises the temperature of the specimen. The fluctuation in grain-size distribution also affects the actual melting point of the individual atoms at boundaries of grains of different sizes. These factors may explain why the

NW becomes thinner and thinner when it is being stretched at a broad temperature range.

High-pressure x-ray diffraction has revealed that the compressibility (extensibility) of alumina<sup>30</sup> and PbS (Ref. 31) solid increases, whereas the Young's modulus decreases as the solid size is decreased.<sup>30</sup> At a certain size, the hardness of the nanosolid decreases as the measuring temperature increases.<sup>32</sup> At high temperatures ( $T > 0.7T_m$ ), the mechanical strength (stress) decreases rapidly with increasing temperature and decreasing strain rate.<sup>33</sup> Superplasticity, that is, an excess strain of  $10^3$  without any substantial necking region when loaded in tension, is generally observed in materials with grain size less than 10 nm in the temperature range  $(0.5-0.6)T_m$ .<sup>34</sup> At large grain boundary area and high self-diffusivity, superplasticity is achievable at lower temperatures and/or higher strain rates for some nanocrystalline materials. Agreement between the predicted trends in Fig. 3 and these observations evidence sufficiently the  $(x_m - x)$  dependent solutions that have covered essential factors such as the size-dependent melting point, specific heat, and bond contraction for the extensibility. One could not expect to cover the fluctuations of mechanical (strain rate), thermal (bombardment or self-heating during process), or grain-size distributions in a theory model, as these fluctuations are artifacts of experiment, though they may become dominant occasionally.

#### IV. CONCLUSION

In summary, we have derived an analytical form for the atomic distance with and without thermal and mechanical

stimuli as well as the extensibility for metallic NW's based on the fact that a molten phase is extremely compressible.<sup>30-32</sup> We can conclude the following.

(1) The extensibility and the maximal strain of a MC depend inapparently on the mechanical stress but apparently on the separation between the melting point and the operating temperature. If the separation approaches zero, the extensibility and the maximal strain approach infinity.

(2) Reconciliation of divergent values on Au-MC stretching limit at various temperatures suggests that the divergence in measurement arises from the thermal and mechanical fluctuations rather than artificially inserted impurity atoms.

(3) For a nanograined nanowire, the bond unfolding and sliding dislocations of the lower-coordinated atoms at grain boundaries are suggested to dominate the high ductility, as the bond stretching limit at temperature approaching the melting point is lower than 150%. The CN-imperfection lowered atomic cohesion takes the responsibility for grain boundary activities.

(4) Understanding suggests that at very low temperatures, a nanosolid should be fragile with lower extensibility, whereas at  $T$  around the surface melting or higher, the nanosolid should be ductile. The melting point of the curved surface of nanosolid drops with decreasing solid size and surface curvature.

Consistency between predictions and observations evidences the impact of atomic CN imperfection on the ductility of a nanosolid and the validity and reality of the BOLS extension that could provide consistent and deeper insight into the unusual behavior of a MC and a NW.

\*FAX: 65 6792 0415. Email address: ecqsun@ntu.edu.sg; URL: <http://www.ntu.edu.sg/home/ecqsun/>

<sup>1</sup>R. Z. Valiev, R. K. Islamgaliev, and I. V. Alexandrov, *Prog. Mater. Sci.* **45**, 103 (2000).

<sup>2</sup>Y. Takai, T. Kawasaki, Y. Kimura, T. Ikuta, and R. Shimizu, *Phys. Rev. Lett.* **87**, 106105 (2001).

<sup>3</sup>A. I. Yanson, G. Rubio-Bollinger, H. E. van den Brom, N. Agraït, and J. M. van Ruitenbeek, *Nature (London)* **395**, 783 (1998).

<sup>4</sup>H. Ohnishi, Y. Kondo, and K. Takayanagi, *Nature (London)* **395**, 780 (1998).

<sup>5</sup>S. B. Legoas, D. S. Galvao, V. Rodrigues, and D. Ugarte, *Phys. Rev. Lett.* **88**, 076105 (2002).

<sup>6</sup>C. Untiedt, A. I. Yanson, R. Grande, G. Rubio-Bollinger, N. Agraït, S. Vieira, and J. M. van Ruitenbeek, *Phys. Rev. B* **66**, 085418 (2002).

<sup>7</sup>S. R. Bahn and K. W. Jacobsen, *Phys. Rev. Lett.* **87**, 266101 (2001).

<sup>8</sup>M. R. Sørensen, M. Brandbyge, and K. W. Jacobsen, *Phys. Rev. B* **57**, 3283 (1998); J. A. Torres, E. Tosatti, A. Dal Corso, F. Ecorcolessi, J. J. Kohanoff, T. D. Di Tolla, and J. M. Soler, *Surf. Sci.* **426**, L441 (1999); D. Sánchez-Portal, E. Artacho, J. Junquera, P. Ordejón, A. Garcia, and J. M. Soler, *Phys. Rev. Lett.* **83**, 3884 (1999); H. Häkkinen, R. N. Barnett, A. G. Scherbakov, and U. Landman, *J. Phys. Chem. B* **104**, 9063 (2000).

<sup>9</sup>G. Rubio-Bollinger, S. R. Bahn, N. Agraït, K. W. Jacobsen, and S. Vieira, *Phys. Rev. Lett.* **87**, 026101 (2001).

<sup>10</sup>F. D. Novaes, A. J. R. da Silva, E. Z. da Silva, and A. Fazzio, *Phys. Rev. Lett.* **90**, 036101 (2003).

<sup>11</sup>L. Lu, M. L. Sui, and K. Lu, *Science* **287**, 1463 (2000).

<sup>12</sup>Y. M. Wang, E. Ma, and M. W. Chen, *Appl. Phys. Lett.* **80**, 2395 (2002).

<sup>13</sup>C. Q. Sun, *Phys. Rev. B* **69**, 045105 (2004).

<sup>14</sup>L. K. Pan, C. Q. Sun, B. K. Tay, T. P. Chen, and S. Li, *J. Phys. Chem. B* **106**, 11 725 (2002).

<sup>15</sup>C. Q. Sun, W. H. Zhong, S. Li, B. K. Tay, H. L. Bai, and E. Y. Jiang, *J. Phys. Chem. B* **108**, 1080 (2004).

<sup>16</sup>H. T. Huang, C. Q. Sun, T. S. Zhang, and P. Hing, *Phys. Rev. B* **63**, 184112 (2000).

<sup>17</sup>C. Q. Sun, H. L. Bai, B. K. Tay, S. Li, and E. Y. Jiang, *J. Phys. Chem. B* **107**, 7544 (2003).

<sup>18</sup>L. K. Pan, C. Q. Sun, and C. M. Li, *J. Phys. Chem. B* **108**, L3404 (2004).

<sup>19</sup>C. Q. Sun, H. L. Bai, S. Li, B. K. Tay, and E. Y. Jiang, *Acta Mater.* **52**, 501 (2004).

<sup>20</sup>C. Q. Sun, Y. Wang, B. K. Tay, S. Li, H. Huang, and Y. B. Zhang, *J. Phys. Chem. B* **106**, 10 701 (2002).

<sup>21</sup>U. F. Kocks, A. S. Argon, and A. S. Ashby, *Prog. Mater. Sci.* **19**, 1 (1975).

- <sup>22</sup>K. K. Nanda, S. N. Sahu, and S. N. Behera, *Phys. Rev. A* **66**, 013208 (2002).
- <sup>23</sup><http://www.svce.ac.in/~msubbu/FM-WebBook/Unit-I/Compressibility.htm>
- <sup>24</sup>C. Q. Sun, *Prog. Mater. Sci.* **48**, 521 (2003).
- <sup>25</sup>J. G. Dash, *Rev. Mod. Phys.* **71**, 1737 (1999).
- <sup>26</sup>R. H. Smit, C. Untiedt, A. I. Yanson, and J. M. van Ruitenbeek, *Phys. Rev. Lett.* **87**, 266102 (2001).
- <sup>27</sup>Y. Champion, C. Langlois, S. Gue'rin-Mailly, P. Langlois, J.-L. Bonnetien, and M. J. Hytch, *Science* **300**, 310 (2003).
- <sup>28</sup>H. Reiss and I. B. Wilson, *J. Colloid Sci.* **3**, 551 (1948); H. Sakai, *Surf. Sci.* **351**, 285 (1996); A. R. Ubbelohde, *The Molten State of Matter* (Wiley, New York, 1978); C. R. M. Wronski, *J. Appl. Phys.* **18**, 1731 (1967); K. J. Hanszen, *Z. Phys.* **157**, 523 (1960).
- <sup>29</sup>Q. Jiang, H. X. Shi, and M. J. Zhao, *Chem. Phys.* **111**, 2176 (1999); M. J. Wautelet, *J. Phys. D* **24**, 343 (1991).
- <sup>30</sup>B. Chen, D. Penwell, L. R. Benedetti, R. Jeanloz, and M. B. Kruger, *Phys. Rev. B* **66**, 144101 (2002).
- <sup>31</sup>S. B. Qadri, J. Yang, B. R. Ratna, E. F. Skelton, and J. Z. Hu, *Appl. Phys. Lett.* **69**, 2205 (1996).
- <sup>32</sup>N. Ono, R. Nowak, and S. Miura, *Mater. Lett.* **58**, 39 (2004).
- <sup>33</sup>N. Agra, A. L. Yeyati, and J. van Ruitenbeek, *Phys. Rep.* **377**, 81 (2003).
- <sup>34</sup>K. S. Siow, A. A. O. Tay, and P. Oruganti, *Mater. Sci. Technol.* **20**, 285 (2004).